Copy
RM L58B27

N 65-33269

(ACCESSION NUMBER) 20		(THRU) /
(PAGES)		(CODE) 01
(NASA CR OR TMX OR AD NUMBER)		(CATEGORY)

FACILITY FORM 602

INVESTIGATION OF AN ALL-MOVABLE CONTROL SURFACE AT

A MACH NUMBER OF 6.86 FOR POSSIBLE FLUTTER

By William T. Lauten, Jr., Gilbert M. Levey,
and William O. Armstrong

Langley Aeronautical Laboratory
Langley Field, Va.

Declassified by authority of NASA
Classification Change Notices No. 2-40
Dated ** 9-15-65

GPO PRICE $

CSFTI PRICE(S) $

Hard copy (HC) 1.00

Microfiche (MF) .50

ff 653 July 65

...ONAL ADVISORY COMMITTEE

FOR AERONAUTICS

WASHINGTON

May 8, 1958

NATIONAL ADVISORY COMMITTEE FOR AERONAUTICS

RESEARCH MEMORANDUM

INVESTIGATION OF AN ALL-MOVABLE CONTROL SURFACE AT

A MACH NUMBER OF 6.86 FOR POSSIBLE FLUTTER

By William T. Lauten, Jr., Gilbert M. Levey,
and William O. Armstrong

SUMMARY

Results of tests for possible flutter of a dynamically and elastically scaled model of a proposed all-movable horizontal tail surface for the North American X-15 airplane are presented herein. Tests at a Mach number of 6.86 were made on the scaled model and on several other configurations having lower stiffnesses. No flutter was obtained. Flexibility influence coefficients and calculated modes and frequencies for the weakest configuration are presented. Calculations of flutter speed of the weakest configuration (piston-theory aerodynamic forces, calculated mode shapes, and experimentally determined frequencies in a modal-analysis calculation scheme being used) yielded a flutter speed approximately four times as high as the velocity obtained in the tests.

INTRODUCTION

Recent developments in aircraft and missiles with all-movable controls have led to increased interest concerning the flutter of such plan forms. Current design trends indicate the need for flutter information on all-movable plan forms at hypersonic speeds. Reference 1 reports tests of a research program in which a rectangular-plan-form, all-movable control was tested at a Mach number of 6.86.

As a part of a program of flutter testing of the various surfaces of the North American X-15 airplane, tests were made in the Langley 11-inch hypersonic tunnel on a 1/12-size model, dynamically and elastically scaled on the basis of dynamic pressure, of a proposed horizontal tail surface. In addition to the scaled model, several configurations with reduced panel and mounting stiffnesses were tested.

Presented herein are the test conditions during the tunnel runs, the structural characteristics of the various configurations, and, for the

weakest configuration, the measured flexibility influence coefficients
and mode shapes and frequencies calculated from the influence coeffi-
cients. The results of flutter calculations on the weakest configura-
tion are included. These calculations were made by using piston-theory
aerodynamic forces (ref. 2), the first three calculated mode shapes, and
the corresponding experimentally determined natural frequencies.

SYMBOLS

a   velocity of sound, fps

f   frequency, cps

g   damping coefficient, theoretical value needed to produce
                 flutter

M   Mach number

q   dynamic pressure, lb/sq ft

ρ air density, slugs/cu ft

Subscripts:

1,2,3,4   indicate natural vibration mode in order of ascending
                 frequency

exp   experimental

calc   calculated

MODEL DESCRIPTION

The model of the all-movable control surface was 1/12 scale with
an exposed-surface aspect ratio of approximately 2.5, a taper ratio
of 0.305, and a sweep angle of 45° at the quarter-chord line. The air-
foil was an NACA 66A005 modified so that it was 1 percent thick at the
trailing edge with a straight-line fairing to the point of tangency.
The airfoil ordinates are listed in table I.

A top-view drawing of the model mounted in the test section is shown
in figure 1(a). Figure 1(b) shows a three-dimensional sketch of the
detail of the spindle and spring restraints. The model was supported in
its base block by means of two flexure springs attached to the spindle in

such a way that the flexure springs provided the same restraint points
as the spindle bearings in the prototype. The flexure spring pivot was
at 25 percent of the mean aerodynamic chord. A third spring, similar to
the flexure springs, was mounted ahead of the model spindle and attached
to the spindle with a screw as shown in figure 1(b). This spring provided
additional pitch stiffness and is referred to as the pitch spring. The
stiffness of the three springs combined to simulate the actuator stiff-
ness of the prototype.

Several configurations were tested. The basic model was dynamically
and elastically scaled from the prototype, both in panel stiffness and
spindle restraint, on the basis of dynamic pressure. The model wing
consisted of a solid aluminum spar, on which the thickness was varied
to obtain the desired stiffness distribution, and five hollow aluminum
streamwise segments, as shown in figure 2. The spar had an integral
spindle for mounting. Each segment was fitted to the spar and fastened
in place with two screws in such a way that the wing stiffness was deter-
mined by the spar stiffness with the segments contributing a negligible
amount. This model is referred to as model I in table II.

Several weaker configurations were tested. Model II had the same
construction as model I except that a hollow spar was used which had
about two-thirds the stiffness of the spar of model I. Model III was
the same as model II except the slots between the segments were covered
over with fiber-glass tape. This resulted in a somewhat stiffer panel.
Model IV was identical to model I except that the spar was drilled out
with 0.1875-inch-diameter holes 0.244 inch on center in order to reduce
the stiffness further. This method of controlling stiffness is discussed
in detail in reference 3. Model V was a modification of model IV in that
the holes were enlarged to 0.204 inch and the spindle was milled so that
its calculated stiffness was cut in half. Figure 3 shows the final spar
and spindle for model V. The small holes in the edges and tip were an
attempt to obtain a more uniform stiffness and mass distribution. The
frequency spectrum of model V indicated that it had about one-fourth the
stiffness of model I.

The model base block, shown in figure 1, served as a model mount
and also as a spacer to support the model in the airstream beyond the
tunnel-wall boundary layer. A reflection plane, also shown in figure 1,
was attached to the model base block just inboard of the wing root. A
photograph of the model mounted in the tunnel is shown in figure 4.

INSTRUMENTATION

A recording oscillograph was used to obtain continuous records during each test from strain gages oriented on the model spar to record strain about two axes (primarily panel bending and torsion) and from a strain gage mounted on the pitch spring. Simultaneously recorded were the outputs from a thermocouple and a pressure cell from which tunnel stagnation temperature and pressure could be determined. Motion pictures at a speed of 128 frames per second were taken of the model during each tunnel run.

LABORATORY MEASUREMENTS

As a preliminary to each tunnel run the frequencies and node lines for the first four natural vibration modes were determined by use of an acoustic shaker. Figure 5 shows a typical set of node lines.

In addition to the natural frequencies of all models, flexibility influence coefficients were determined prior to testing for models IV and V (runs 9 and 11). The location of the points at which the models were loaded is shown in figure 6. The influence coefficients for model V (the weakest model) are tabulated in table III with the calculated mode shapes and frequencies for the first three natural modes. Also listed are the experimentally determined frequencies.

The wing deflections were measured electrically by an array of differential transformers. These transformers were connected to a null balance indicator with a visual indication which could be read to 0.0001 inch. This system was accurate to ±0.001 inch from 25 to 75 percent of full range; however, for reading small differences, for example, the difference between 0.0550 and 0.0560 inch, the readings could be repeated to at least ±0.0001 inch.

The mass, center of gravity, and moment of inertia of each of the five wing segments were determined experimentally. The corresponding quantities for the portion of the spar of model V associated with each segment were calculated. Then, in order to meet the requirement for correct total mass, center of gravity, and moment of inertia of any streamwise segment while still associating two masses with the loading points of that segment, a fictitious mass was assigned to each segment at the locations shown in figure 6. The displacement associated with each such mass was found by linear interpolation between the loading points of that segment. This results in dynamic coupling terms in the mass matrix. (See table IV.) These terms are similar to those introduced by Rodden in reference 4 and, while satisfying the three known conditions
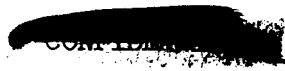
of mass, center of gravity, and moment of inertia of a strip, give the proper kinetic energy of the vibrating strip.

TEST PROCEDURE

The tests were made in the Langley 11-inch hypersonic tunnel by using a single-step, two-dimensional Invar nozzle. With this nozzle, the tunnel operates at an average Mach number of 6.86. A description of the tunnel is given in reference 5 and a preliminary calibration of the Invar nozzle is included in reference 6.

In an effort to determine a flutter boundary, the density in the test section was increased during each run by gradually increasing the stagnation pressure from 5 atmospheres to a peak value of about 38 atmospheres. For normal runs, about 30 seconds were required for the dynamic pressure to reach a maximum value.

In order to alleviate the danger of damage to the model by the starting and stopping transients, restraining pins, operated by a lever outside the tunnel, were inserted into the root section until the starting shock passed through the test section, were retracted during the increase to maximum pressure, and were reinserted before the tunnel closed down.

There was deviation from the normal testing procedure on three of the tests. In run 6, the tunnel was started at maximum stagnation pressure - 42 atmospheres; in run 7, the wing was preloaded at the tip and released suddenly when the tunnel reached near maximum pressure; and in run 10, the model was tested at an angle of attack of about $2\frac{1}{2}^{\circ}$. None of these variations had any apparent effect on the model stability.

RESULTS AND DISCUSSION

A summary of the test results is given in table II, which lists the first four natural frequencies, test-section density, speed of sound, and dynamic pressure at maximum pressure test condition and presents brief explanatory remarks for each run. No flutter was obtained on any of the configurations tested.

Since reference 1 reported good agreement between calculated and experimental flutter speed at the test Mach number, it was felt worthwhile to make the same calculation on model V reported here. The calculations were made by using the aerodynamic forces derived from piston

theory (ref. 2), the first three coupled vibration modes as calculated from the influence coefficients, and the experimentally determined frequencies for these modes in a modal-analysis calculation scheme. The effects of thickness were included. This calculation yielded a result that may be interpreted alternatively as follows: (1) The flutter speed was about four times the maximum speed reached in the test or (2) the stiffness of model V would have to be decreased by a factor of approximately 16 before flutter could be expected to occur. This reduction would have been impractical with the model as originally constructed. The results of these calculations are presented in figure 7 in the form of a plot of velocity against damping coefficient for the only mode of vibration that had an instability. The damping coefficient g was assumed to have the same value for all modes and provides for theoretical or actual damping forces as illustrated, for example, in section 8.1 of reference 7.

CONCLUDING REMARKS

Flutter tests at a Mach number of 6.86 of a dynamically and elastically scaled model of a sweptback, all-movable horizontal tail proposed for the North American X-15 airplane and on several configurations having lower stiffnesses are reported. The spectrum of natural vibration frequencies indicates that the weakest configuration was one-fourth as stiff as the stiffest configuration. No flutter was obtained.

Langley Aeronautical Laboratory,
    National Advisory Committee for Aeronautics,
   Langley Field, Va., February 12, 1958.

REFERENCES

1. Runyan, Harry L., and Morgan, Homer G.: Flutter at Very High Speeds. NACA RM L57D16a, 1957.

2. Ashley, Holt, and Zartarian, Garabed: Piston Theory - A New Aerodynamic Tool for the Aeroelastician. Jour. Aero. Sci., vol. 23, no. 12, Dec. 1956, pp. 1109-1118.

3. Land, Norman S., and Abbott, Frank T., Jr.: Method of Controlling Stiffness Properties of a Solid-Construction Model Wing. NACA TN 3423, 1955.

4. Rodden, W. P.: A Matrix Approach to Flutter Calculations. Rep. No. NA-56-1070, North American Aviation, Inc., May 1, 1956.

5. McLellan, Charles H., Williams, Thomas W., and Beckwith, Ivan E.: Investigation of the Flow Through a Single-Stage Two-Dimensional Nozzle in the Langley 11-Inch Hypersonic Tunnel. NACA TN 2223, 1950.

6. Bertram, Mitchell H.: Exploratory Investigation of Boundary-Layer Transition on a Hollow Cylinder at a Mach Number of 6.9. NACA Rep. 1313, 1957. (Supersedes NACA TN 3546.)

7. Scanlan, Robert H., and Rosenbaum, Robert: Introduction to the Study of Aircraft Vibration and Flutter. The Macmillan Co., 1951.

TABLE I

ORDINATES FOR NACA 66A005 (MODIFIED) AIRFOIL

$\left[\text{Ordinates in percent of chord}\right]$

x	$y_U = y_L$
0	0
.10	.269
.25	.408
.50	.531
.75	.590
1.25	.650
2.50	.791
5.00	1.048
7.50	1.270
10.00	1.460
15.00	1.766
20.00	2.001
25.00	2.182
30.00	2.318
35.00	2.416
40.00	2.476
45.00	2.500
50.00	2.488
55.00	2.438
60.00	2.346
65.00	2.176
[a]67.00	2.085
100.00	.500
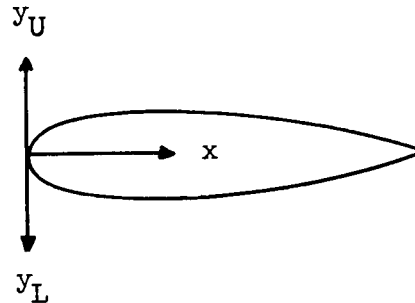
[a]Straight-line fairing from 67 to 100 percent chord.

TABLE II

EXPERIMENTAL DATA

Run	Model	f_1, cps	f_2, cps	f_3, cps	f_4, cps	ρ, slugs/cu ft	a, fps	q, lb/sq ft	Remarks
1	I	88	263	293	461	0.000128	506	769	Solid spar and stiffest pitch spring
2	IA	88	258	289	475	.000110	528	724	Solid spar and weakened pitch spring
3	IB	87	254	287	479	.000111	521	707	Solid spar and no pitch spring
4	II	82	224	252	392	.000108	531	719	Hollow spar and no pitch spring for rest of runs
5	IIA	79	207	251	385	.000115	522	735	Hollow spar, reduced flexure stiffness
6	IIA	79	207	251	385	.000134	500	793	Same as run 5, except run started at maximum density
7	IIA	79	207	251	385	.000129	512	794	Same as run 5, but model excited during run
8	III	83	227	309	580	.000128	480	692	Same as run 5, but slots taped over
9	IV	54	138	220	319	.000126	496	730	Solid spar drilled with 0.1875-inch-diameter holes
10	IV	54	138	220	319	.000119	500	702	Same as run 9 but model at angle of attack of $2\frac{1}{2}^{\circ}$
11	V	44	115	148	172	.000112	521	713	Holes in spar enlarged to 0.204 inch in diameter, and spindle stiffness decreased

TABLE III

MEASURED FLEXIBILITY INFLUENCE COEFFICIENTS AND CALCULATED-MODE-SHAPE

VALUES AT STATIONS INDICATED IN FIGURE 6 FOR MODEL V

Loading station	Deflections for 500-gram load, in inches, at station -									
	1	2	3	4	5	6	7	8	9	10
1	0.0747	0.0353	0.0124	-0.0018	-0.0085	0.0826	0.0537	0.0310	0.0145	0.0096
2	.0353	.0250	.0091	-.0003	-.0047	.0407	.0290	.0185	.0093	.0050
3	.0124	.0091	.0055	.0020	-.0011	.0141	.0091	.0058	.0035	.0012
4	-.0018	-.0003	.0020	.0031	.0022	-.0034	-.0019	-.0012	-.0010	-.0011
5	-.0085	-.0047	-.0011	.0022	.0071	-.0140	-.0103	-.0074	-.0053	-.0045
6	.0826	.0407	.0141	-.0034	-.0140	.1134	.0750	.0445	.0236	.0090
7	.0537	.0290	.0091	-.0019	-.0103	.0750	.0515	.0313	.0166	.0081
8	.0310	.0185	.0058	-.0012	-.0074	.0445	.0313	.0224	.0121	.0070
9	.0145	.0093	.0035	-.0010	-.0053	.0236	.0166	.0121	.0081	.0054
10	.0096	.0050	.0012	-.0011	-.0045	.0090	.0081	.0070	.0054	.0031

Loading station	First mode	Second mode	Third mode
1	0.73297	1.00000	1.00000
2	.39308	.42242	.99770
3	.12749	.32034	.56289
4	-.03655	.32664	.22615
5	-.16073	.77199	.01802
6	1.00000	.98218	-.52444
7	.68561	.35259	-.18950
8	.43781	-.22534	.04130
9	.24328	-.47219	.03520
10	.12744	-.54264	.26679
f_{calc}, cps	40.5	110.0	163.4
f_{exp}, cps	44	115	148

TABLE IV

MASS MATRIX WITH DYNAMIC COUPLING TERMS

$$\left[\text{Mass in slugs}\right]$$

Station	1	2	3	4	5	6	7	8	9	10
1	0.0005668	0.	0	0	0	-0.0006818	0	0	0	0
2	0	0.0009409	0	0	0	0	-0.0010145	0	0	0
3	0	0	0.0014018	0	0	0	0	-0.0015243	0	0
4	0	0	0	0.0019498	0	0	0	0	-0.0021861	0
5	0	0	0	0	0.0025899	0	0	0	0	-0.0032467
6	-0.0006818	0	0	0	0	0.0010095	0	0	0	0
7	0	-0.0010145	0	0	0	0	0.0016016	0	0	0
8	0	0	-0.0015243	0	0	0	0	0.0023088	0	0
9	0	0	0	-0.0021861	0	0	0	0	0.0032115	0
10	0	0	0	0	-0.0032467	0	0	0	0	0.0043711
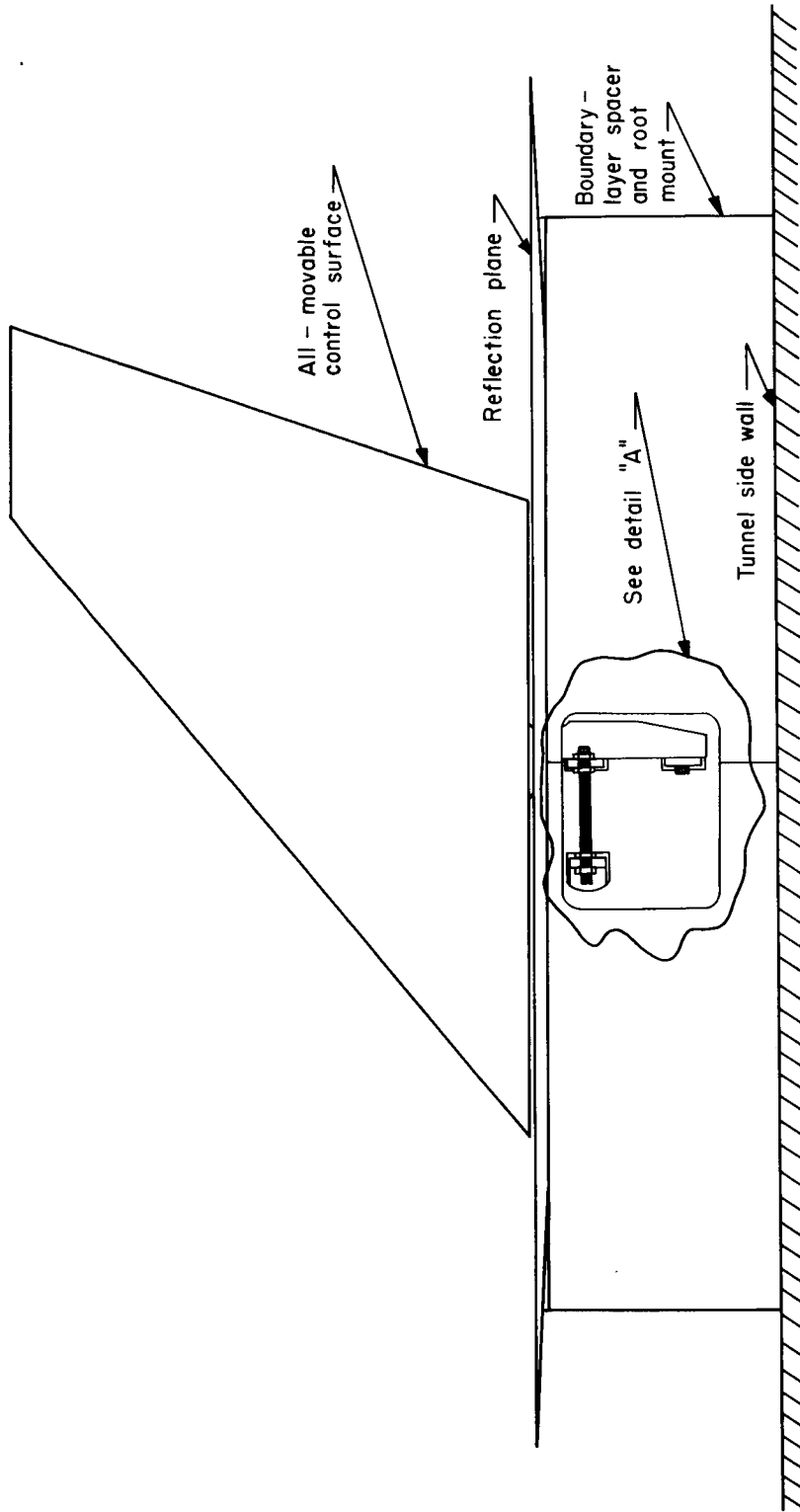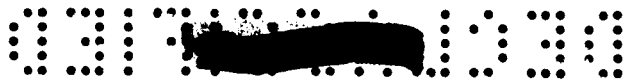
(a) Overall view.

Figure 1.- Top view of wing as mounted in the tunnel.
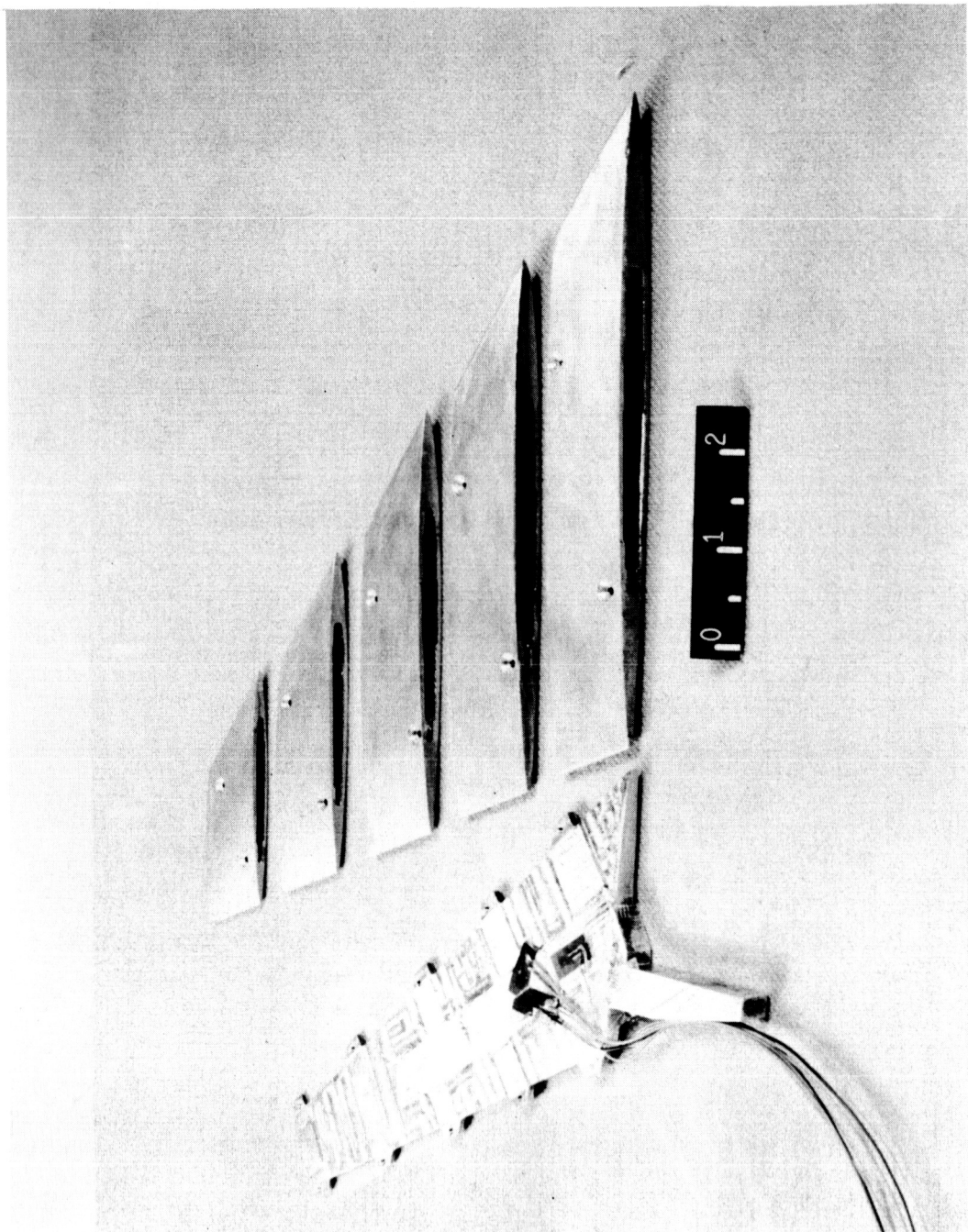
DECLASSIFIED

Spindle

Flexures
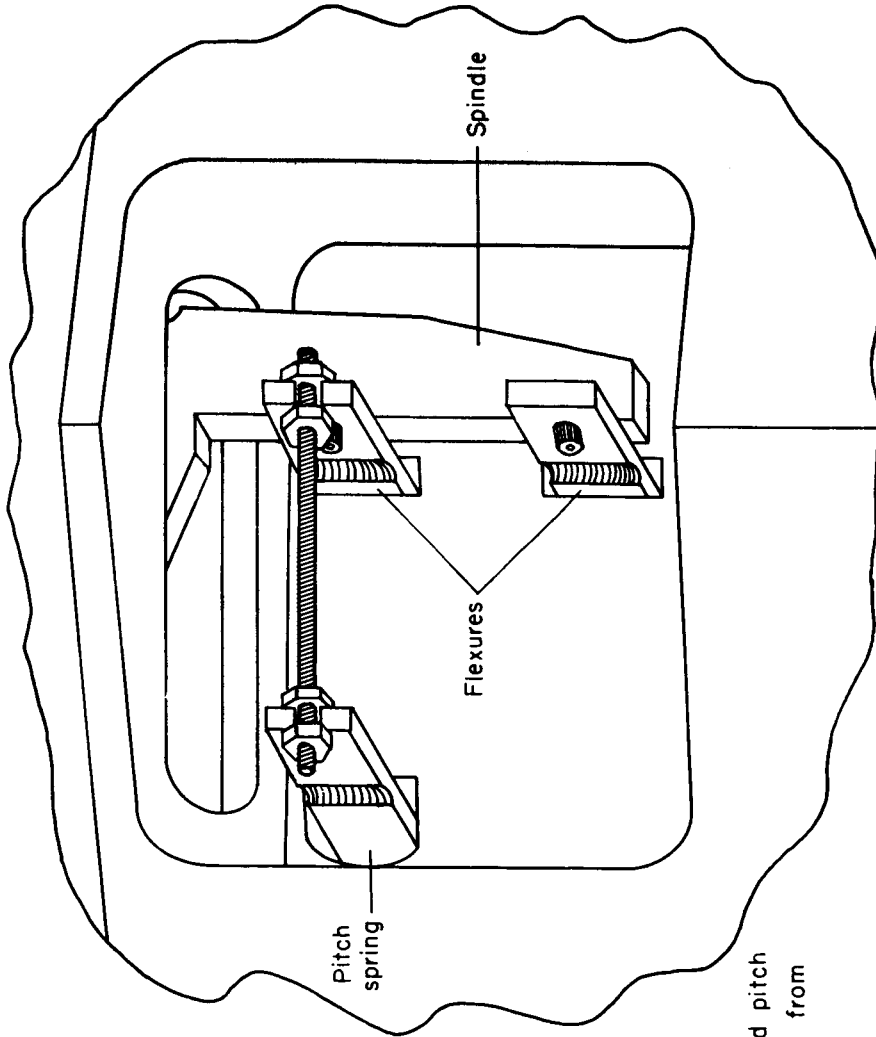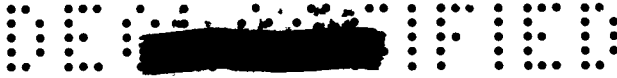
Pitch
spring

Note: Flexures and pitch
spring cantilevered from
lower surface.

Detail "A"

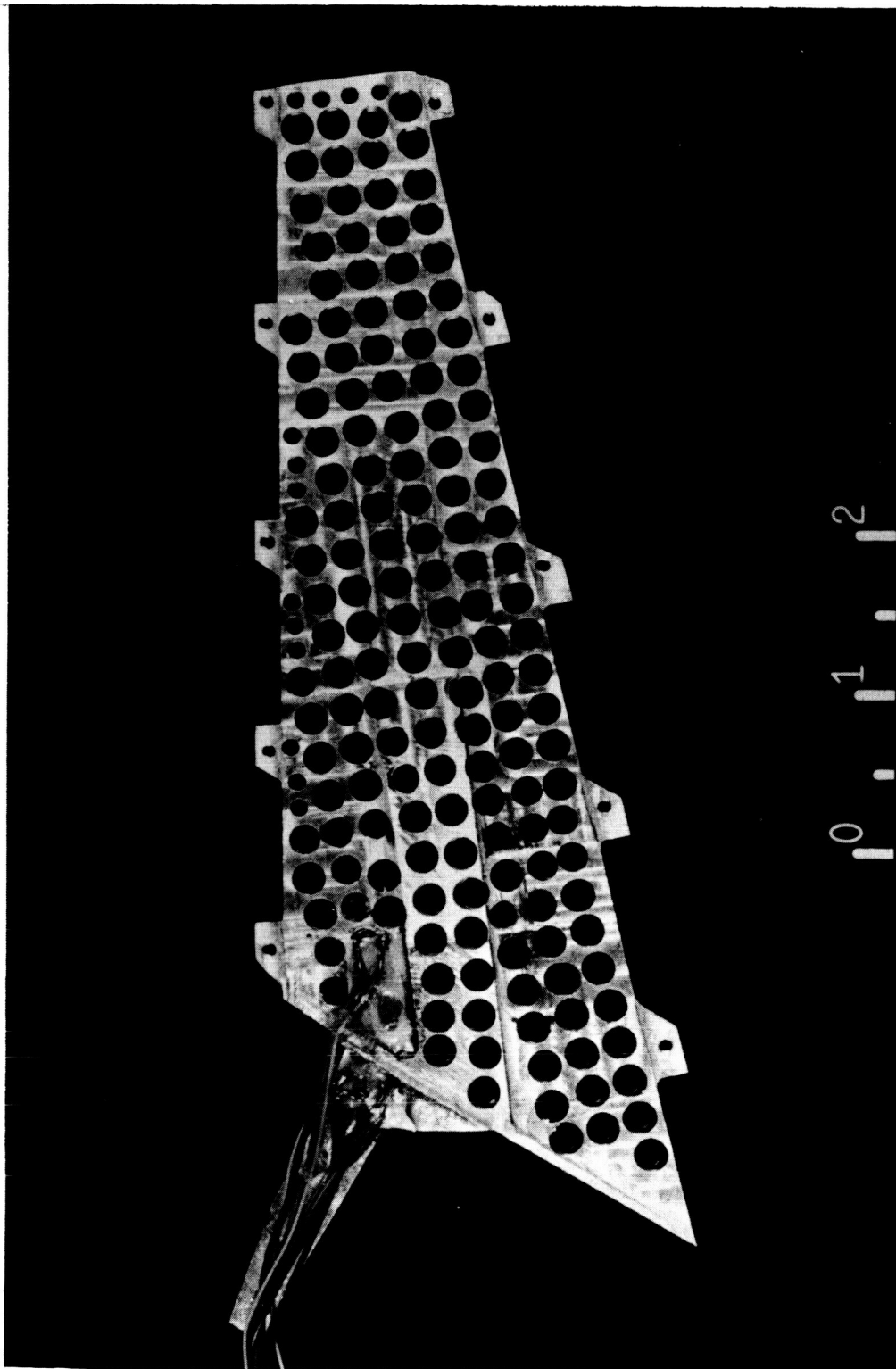(b) Sketch showing detail of spindle support system.

Figure 1.- Concluded.

L-57-2178

Figure 2.- Photograph of solid-spar model with segments detached.

DEC▮▮▮IFIED

L-57-2207

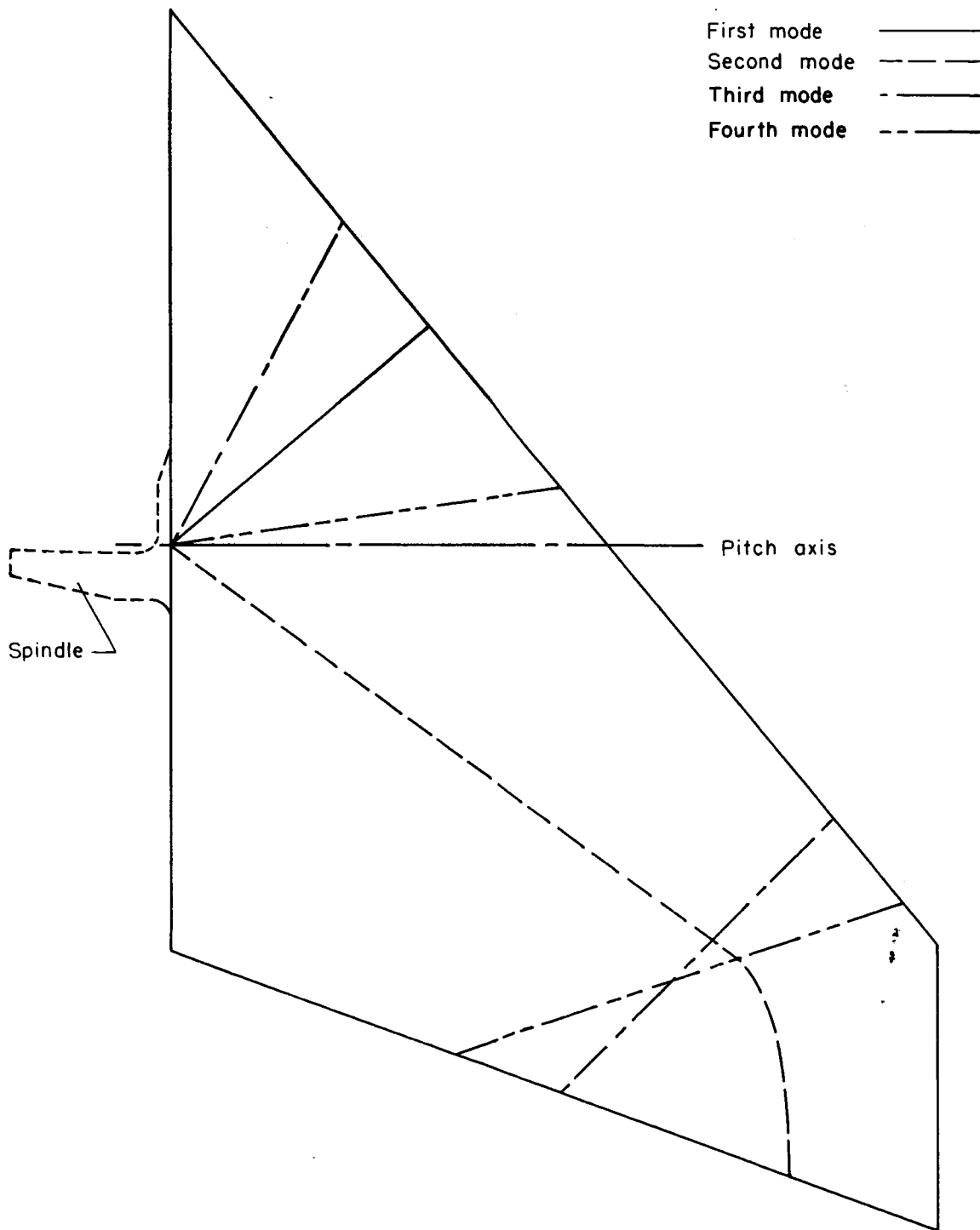Figure 3.- Photograph of solid spar showing hole pattern for model V.

L-57-2177

Figure 4.- Photograph of model mounted in tunnel showing reflection plane.

First mode ——————
Second mode —— — —
Third mode - ————
Fourth mode —— ————

Pitch axis

Spindle

Figure 5.- Sketch of model showing typical nodal patterns.
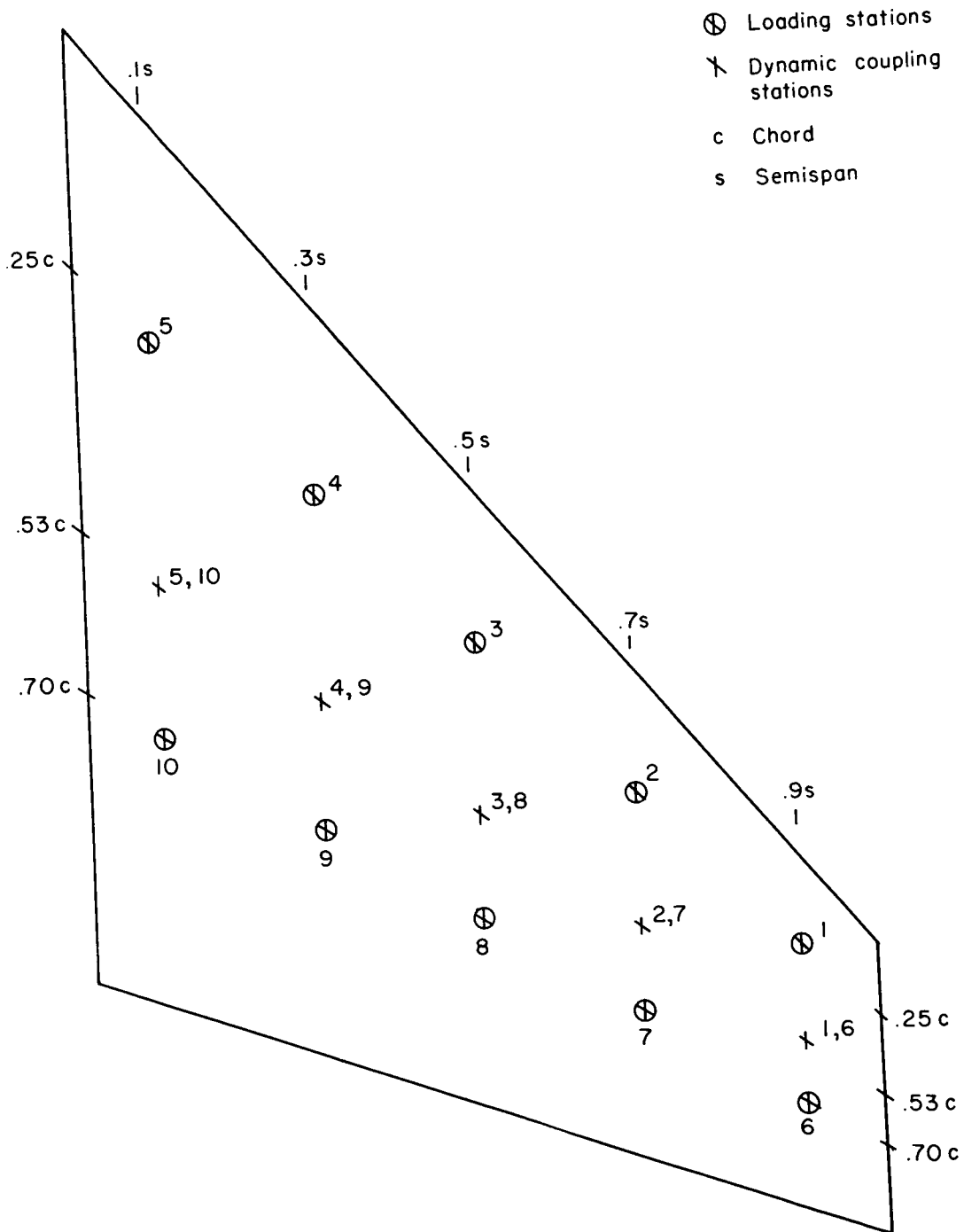
Figure 6.- Sketch of model showing points of load application and measurement of flexibility influence coefficients and the location of fictitious masses that are used in the analytical solution.
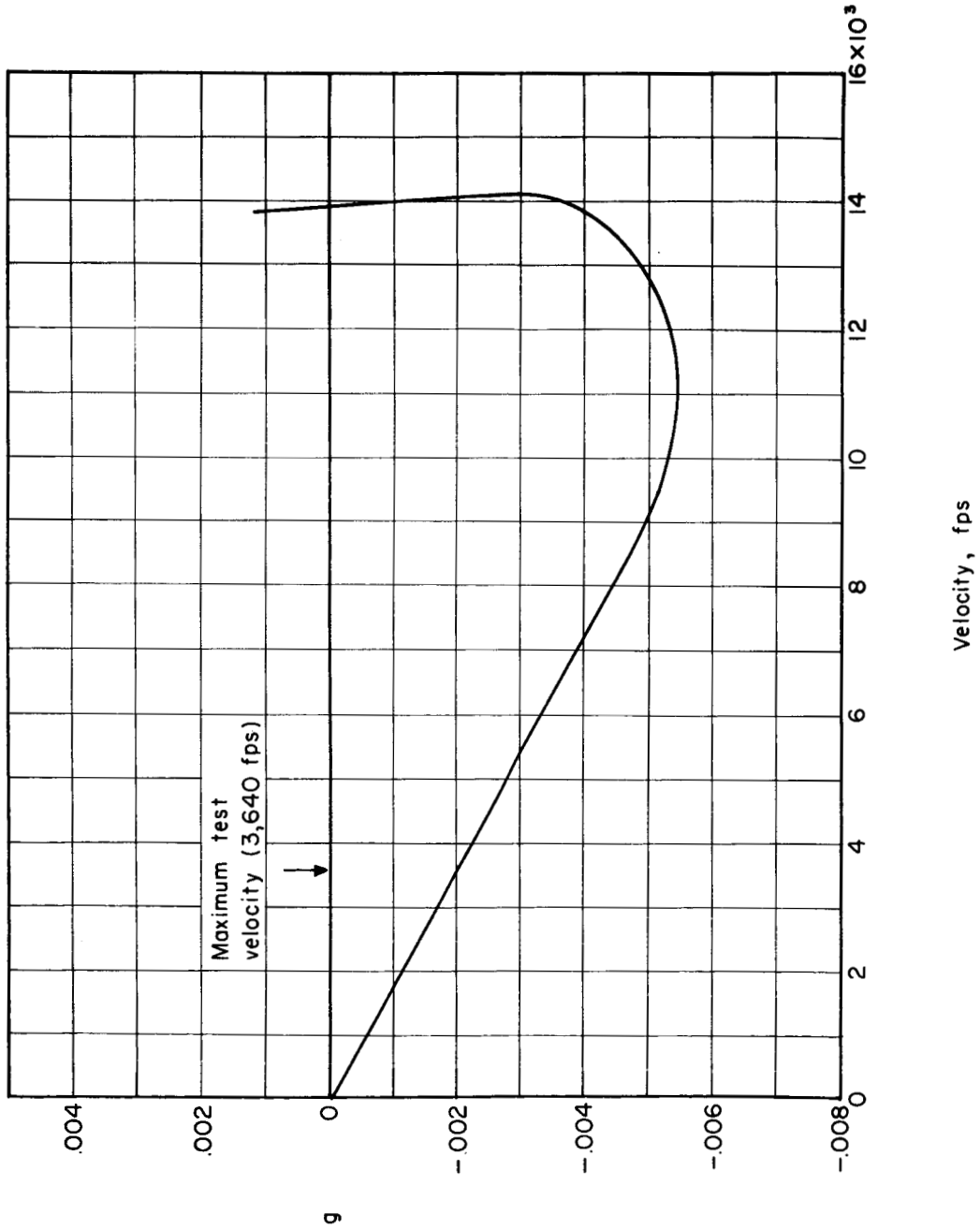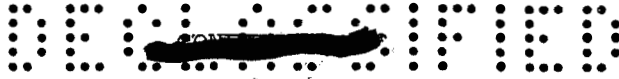
DECLASSIFIED

Figure 7.- Plot of velocity against damping coefficient for the only unstable vibration mode.